Vol. 24, No. 2(2025) Proc25524

Revista Mexicana de Ingeniería Química

Evaluation of the presence of metallic cations (Cu^{2+}, Zn^{2+}, Fe^{2+}, Pb^{2+}) in silver sulfide leaching with thiosulfate: Thermodynamic and experimental study

Evaluación de la presencia de cationes metálicos (Cu^{2+}, Zn^{2+}, Fe^{2+}, Pb^{2+}) en la lixiviación de sulfuro de plata con tiosulfato: Estudio termodinámico y experimental

G. Cisneros-Flores[1], J. C. Juárez-Tapia[1], I. A. Reyes-Domínguez[2], N. Toro[3], G. Urbano-Reyes[1], E. J. Muñoz-Hernández[1], J. I. Martínez-Soto[1], A. M. Teja-Ruíz[4]*

[1] Área Académica de Ciencias de la Tierra y Materiales, Universidad Autónoma del Estado de Hidalgo (UAEH), Pachuca de Soto 42184, México

[2] Catedrático CONACYT-Instituto de Metalurgia, Universidad Autónoma de San Luis Potosí, San Luis Potosí 78210, México

[3]Faculty of Engineering and Architecture, Universidad Arturo Prat, Iquique 1110939, Chile

[4] *Dirección* de Laboratorios, Universidad Autónoma del Estado de Hidalgo (UAEH), Pachuca de Soto 42184, México

Received: February 8, 2025; Accepted: April 20, 2025

Abstract

This study evaluates the effect of Cu^{2+}, Zn^{2+}, Pb^{2+}, and Fe^{2+} on the selective leaching of Ag_2S with thiosulfate. Pourbaix diagrams were used to identify the stability and predominance regions of the species formed as a function of ORP and pH, providing a theoretical framework to predict the influence of each ion. Experimental tests were conducted with high-purity reagents (≥ 99.5%) to isolate the individual effect of each ion without interference from complex matrices. The results showed that Cu^{2+} at low concentrations and Zn^{2+} enhance Ag_2S leaching, while Fe^{2+}, Pb^{2+}, and higher concentrations of Cu^{2+} inhibit the process, exhibiting behavior similar to cyanicide metals. X-ray Diffraction (XRD) analysis allowed the identification of byproducts formed in the solid residues. The correlation between thermodynamic, experimental, and XRD results led to the proposal of reaction mechanisms in the S_2O_3 – Ag_2S – M^{2+} systems, where M represents the analyzed cations. These findings provide fundamental insights into Ag_2S leaching with thiosulfate and its potential application in polymetallic sulfides and precious metal-containing waste.

Keywords: Silver leaching with thiosulfate, Leaching chemistry, Thiosulfate decomposition.

Resumen

Este estudio evalúa el efecto de los cationes Cu^{2+}, Zn^{2+}, Pb^{2+} y Fe^{2+} en la lixiviación selectiva de un sulfuro de plata con tiosulfato. A través del modelado termodinámico mediante diagramas de Pourbaix, se identificaron las zonas de estabilidad y predominio de las especies formadas en función del ORP y pH, proporcionando un marco teórico para predecir la influencia de cada ion en el sistema de lixiviación. Se realizaron pruebas experimentales con reactivos de alta pureza (≥ 99.5%) para aislar el efecto individual de cada ion sin interferencias de matrices complejas. Los resultados revelaron que Cu^{2+} en bajas concentraciones y Zn^{2+} favorecen la lixiviación de Ag_2S, mientras que Fe^{2+}, Pb^{2+} y concentraciones elevadas de Cu^{2+} la inhiben, exhibiendo un comportamiento similar al de los metales cianicidas. Mediante Difracción de Rayos X (DRX), se identificaron los subproductos formados en el residuo sólido. La correlación entre los resultados termodinámicos, experimentales y los difractogramas permitió proponer los mecanismos de reacción en los sistemas S_2O_3 – Ag_2S – M^{2+}, donde M representa los cationes analizados. Estos hallazgos no solo contribuyen a la comprensión fundamental de la lixiviación de Ag_2S con tiosulfato, sino que también proporcionan información relevante para su aplicación en sistemas más complejos, como sulfuros polimetálicos y residuos de metales preciosos.

Palabras clave: Lixiviación de plata con tiosulfato, química de lixiviación, descomposición de tiosulfato.

* *Corresponding author. E-mail*: aislinn_ teja@uaeh.edu.mx ;
https://doi.org/10.24275/rmiq/Proc25524
ISSN:1665-2738, *issn-e*: 2395-8472

1 Introduction

Cyanide has been widely used in the leaching process of precious metals such as gold (Au) and silver (Ag), but it is not without areas for improvement. Cyanide is selective for metals such as copper, zinc, iron, and nickel, among others, significantly increasing its consumption. On the other hand, it is incapable of dissolving refractory minerals, making it ineffective for processing complex ores (Alarcon *et al*., 2018; Liu *et al*., 2023; Soto *et al*., 2023). In addition to these technical limitations, its high toxicity and the associated risks of its use have been the subject of study, as cyanide-related incidents have led to environmental disasters, regulatory restrictions, and increasing public opposition in mining communities (Dwivedi *et al*., 2021; Mitra, 2019). Moreover, the growing demand for Ag and Au, driven by their implementation in a wide variety of everyday products, has caused the overexploitation of primary extraction sources, resulting in their depletion and forcing the min ing industry to face the challenge of processing increasingly complex ores. This has generated growing interest in the processing of alternative sources, such as electronic waste, and mining byproducts, including tailings and concentrates, which contain valuable metals that can be recovered through hydrometallurgical processes (Erust *et al*., 2023; Serga *et al*., 2022). Given these challenges, exploring more sustainable and environmentally friendly leaching agents has become essential. Conventional lixiviants not only exhibit technical limitations but also pose significant environmental and economic concerns, reinforcing the need for alternative approaches not only in leaching agents but also in complementary remediation strategies, such as biosorption and the use of metal-resistant microorganisms (Asencios *et al*., 2022; Cos & Fuentes, 2023; Meléndez *et al*., 2022). Among the alternatives to cyanide, thiosulfate has stood out as one of the most promising leaching agents for precious metals due to its low toxicity and reduced environmental impact. Thiosulfate acts as a bifunctional ligand, coordinating with metals through two types of donor atoms: sulfur (S) and oxygen (O). This characteristic allows it to form stable complexes with various metals following the hard and soft acids and bases theory. Sulfur, being a soft donor, tends to have an affinity for metals such as Au(I) and Ag(I), while oxygen, being a hard donor, binds to metals such as copper and iron (Pearson, 1997; Trachevskii *et al*., 2008). However, one of the main areas of opportunity for the effective use of thiosulfate lies in its excessive oxidative degradation and the complexity of its reaction chemistry (Urzúa *et al*., 2018; Puente *et al*., 2021; Xu *et al*., 2017; Yae *et al*., 2023). Because of this, there is great interest in finding oxidizing agents that promote an optimal ORP, including the use of air and O_2, as well as the implementation of metallic ions such as Cu^{2+}, Zn^{2+}, Co^{3+}, and Fe^{3+} (Juárez-Tapia *et al*., 2012; Puente *et al*., 2017; Zhang *et al*., 2022a, 2022b). However, the use of these oxidizing agents may increase thiosulfate consumption due to their reactivity with these ions, generating undesirable secondary reactions. This behavior is similar to that observed with the so-called cyanicide metals, which also form stable complexes with cyanide and increase its consumption during leaching (Larrabure & Rodríguez, 2021). This study examines the effect of metallic ions (Cu^{2+}, Zn^{2+}, Pb^{2+}, and Fe^{2+}) at various concentrations on the dissolution behavior of silver sulfide in a thiosulfate medium. The objective is to determine whether these ions enhance silver dissolution or, conversely, trigger secondary reactions that compromise thiosulfate stability. Based on this analysis, we aim to establish a classification analogous to cyanicide metals, identifying as *thiosulfacide metals* those that negatively impact the thiosulfate leaching process. Additionally, this study provides insights into reaction mechanisms involved in the leaching of silver sulfide with thiosulfate in the presence of these cations, facilitating the identification of metallic species that may interfere with the recovery of the target metal. This information allows for the design or adjustment of multi-stage leaching processes, where problematic cations are selectively dissolved in an initial phase before implementing thiosulfate leaching (Segura & Lapidus, 2023). This approach optimizes the recovery of the target metal while minimizing adverse effects on the lixiviant. Although the experiments were conducted using synthetic samples to ensure controlled conditions and isolate the specific influence of each metallic ion, the findings provide fundamental insights into the mechanisms governing thiosulfate leaching. This study serves as a valuable reference for future research involving more complex matrices, such as polymetallic ores or secondary metal sources, including electronic waste, where additional interactions may further influence the leaching process.

2 Methods and materials

For this investigation, high-purity reagents were used: silver sulfide (Ag_2S, Sigma-Aldrich ≥99.5%), copper sulfate ($CuSO_4 \cdot 5H_2O$, M&B ≥99.5%), zinc sulfate ($ZnSO_4 \cdot 7H_2O$, J.T. Baker 99.9%), lead sulfate ($PbSO_4$, Analytyka ≥99.5%), ferrous sulfate ($FeSO_4 \cdot 7H_2O$, J.T. Baker 99.9%), and sodium thiosulfate ($Na_2S_2O_3 \cdot 5H_2O$, MEYER ≥99.5%). Deionized water was used in all the experiments.

The thermodynamic analysis was performed prior to the experimental phase to predict the stability of silver-thiosulfate complexes and the potential interactions with Cu^{2+}, Zn^{2+}, Pb^{2+}, and Fe^{2+}. This was achieved through the construction of Eh-pH diagrams using the Hydra MEDUSA Chemistry software, while the thermodynamic constant database was updated with the assistance of HSC Chemistry 6 software. The insights from this analysis guided the selection of key experimental conditions, particularly the pH range (~8), which was chosen to maintain thiosulfate stability while minimizing the formation of undesirable species. Additionally, the thermodynamic predictions regarding the formation of solid phases were later verified through X-Ray Diffraction (XRD) analysis of the leaching residues. Silver sulfide leaching tests were conducted with 0.5 L of an alkaline solution (pH ≈ 8) in a PYREX glass reactor placed on a Thermo Scientific heating plate, which was used to monitor temperature and applied stirring speed. Air was injected through a diffuser and regulated with a flowmeter. During the process, 10 mL aliquots were extracted at predetermined time intervals: 0, 0.5, 1.0, 1.5, 2, 3, 4, 6, 8, 10, 12, and 24 hours. The aliquots were subsequently analyzed by Inductively Coupled Plasma Emission Spectrometry (ICP) using a Perkin Elmer 3000 spectrometer to determine the concentration of Ag in solution. The experimental parameters used in the leaching tests are presented in Table 1. Finally, the solid residues from the leaching process were analyzed by X-Ray Diffraction (XRD) using an INEL EQUINOX 2000 X-ray diffractometer (Thermo Fisher Scientific, Ecublens, Switzerland) with Co-Kα1 radiation (1.789010 Å). The radiation settings were 30 mA, 20 kV, and 220 V, with a resolution of 0.095 FWHM. Phase identification was carried out using Match 3 software with the COD-Inorg REV140301 database.

Table 1 Experimental conditions of the leaching tests.

Parameter	Value
$[CuSO_4 \cdot 5H_2O]$ (g/L)	0.062, 0.187, 0.25, 0.5, 0.75, 1.0
$[PbSO_4]$ (g/L)	0.045, 0.11, 0.22, 0.33, 0.44, 0.55
$[Na_2S_2O_3 \cdot 5H_2O]$ (g/L)	30
$[Ag_2S]$ (g/L)	0.4
$ZnSO_4 \cdot 7H_2O$ (g/L)	0.33, 0.44, 0.55, 1.1, 2.2. 3.3
$FeSO_4 \cdot 7H_2O$ (g/L)	0.25, 0.5, 0.75, 1.0, 1.5, 2.0
Temperature (K)	298
Agitation Speed (RPM)	700
pH	≈ 8
Solution volume (L)	0.5

The experimental pH and temperature conditions were selected based on the literature, which indicates that thiosulfate remains stable at ambient temperature, preventing unnecessary degradation (Alvarado *et al*., 2015). Additionally, it has been reported that pH values exceeding the 8–9 range negatively impact the process by promoting the formation of undesirable species (Deutsch, 2012; Xu *et al*., 2017).

3 Results

3.1 Eh - pH diagrams

The following section presents the thermodynamic analysis of the systems examined in this research by constructing Eh–pH diagrams. In addition, Table 2 shows the reactions involved in the thermodynamic analysis along with their log(K) values, where log(K) represents the logarithm of the equilibrium constant associated with each reaction. These values, determined using HSC Chemistry 6 software, indicate the thermodynamic favorability of the reactions, with higher log(K) values suggesting more spontaneous processes under the studied conditions.

The Pourbaix diagram in Figure 1 illustrates the species present in the thiosulfate–silver medium at different potential and pH values. On one hand, Figure (1a) shows the different by products generated from the oxidative process of thiosulfate, including tetrathionate ($S_4O_6^{2-}$), dithionate ($S_2O_6^{2-}$), and persulfate ($S_2O_8^{2-}$), while Figure (1b) presents the formation of thiosulfate–silver complexes such as $AgS_2O_3^-$ and $Ag(S_2O_3)_2^{3-}$. Additionally, the formation of silver sulfites is observed, including $AgSO_3^-$, $Ag(SO_3)_2^{3-}$, and $Ag(SO_3)_3^{5-}$. Likewise, according to the studies by Melashvili *et al*., 2015, and Ou *et al*., 2023, the oxidation of thiosulfate in the presence of oxygen and in an alkaline medium favors the formation of trithionate and tetrathionate. Both compounds can regenerate thiosulfate molecules, as shown in Eq (2). However, as observed in Eq (3), trithionate leads to the formation of sulfite ions (SO_3^{2-}), which, upon oxidation, are transformed into sulfate (SO_4^{2-}), as described in Eq (4). The latter represents the final product of thiosulfate oxidation.

The Eh–pH diagrams in Figure 2 present the stability regions of the aqueous species in the systems S_2O_3–Ag–Cu^{2+}, S_2O_3–Ag–Zn^{2+}, S_2O_3–Ag–Fe^{2+}, and S_2O_3–Ag–Pb^{2+}. In the S_2O_3–Ag - Cu^{2+} system (Figure 2a), three thiosulfate–silver complexes ($AgS_2O_3^{2-}$, $Ag(S_2O_3)_2^{3-}$, and $Ag(S_2O_3)_3^{5-}$) are identified, with $Ag(S_2O_3)_3^{5-}$ being the predominant species at pH ≈ 8 and under oxidizing potentials, which requires a higher concentration of thiosulfate (Eq 7). As the system's ORP increases, the oxidative degradation of thiosulfate is favored, leading to the formation of species such

Table 2 Equilibrium constants and associated equations of the reactions in the thiosulfate system.

Equation	log (K)	Eq.
$2S_2O_3^{2-} + 0.5O_2 + H_2O \rightarrow S_4O_6^{2-} + 2OH^-$	28.171	(1)
$4S_4O_6^{2-} + 6OH^- \rightarrow 5S_2O_3^{2-} + 2S_3O_6^{2-} + 3H_2O$	10.044	(2)
$2S_3O_6^{2-} + 6OH^- \rightarrow S_2O_3^{2-} + 4SO_3^{2-} + 3H_2O$	55.685	(3)
$SO_3^{2-} + 0.5O_2 \rightarrow SO_4^{2-}$	90.344	(4)
$2S_2O_3^{2-} + Ag^+ \rightarrow Ag(S_2O_3)_2^{3-}$	10.997	(5)
$S_2O_3^{2-} + Ag^+ \rightarrow AgS_2O_3^-$	8.5	(6)
$3S_2O_3^{2-} + Ag^+ \rightarrow Ag(S_2O_3)_3^{5-}$	14.2	(7)
$S_2O_3^{2-} + Ag^+ + 3H_2O \rightarrow 6H^+ + 4e^- + Ag(SO_3)_2^{3-}$	-36.2	(8)
$S_2O_3^{2-} + 2Ag^+ + 3H_2O \rightarrow 6H^+ + 4e^- + 2Ag(SO_3)^-$	-17.09	(9)
$S_2O_3^{2-} + Cu^+ + e^- \rightarrow CuS_2O_3^-$	12.93	(10)
$Cu^{2+} + 2H_2O \rightarrow 2H^+ + Cu(OH)_2$	-6.401	(11)
$Cu^{2+} + 3H_2O \rightarrow 3H^+ + Cu(OH)_3^-$	-25.38	(12)
$S_2O_3^{2-} + 2Cu^{2+} + 3H_2O \rightarrow 6H^+ + 2e^- + 2CuSO_3^-$	-12.06	(13)
$S_2O_3^{2-} + Cu^{2+} + 3H_2O \rightarrow 6H^+ + 3e^- + 2Cu(SO_3)_2^{3-}$	-33.95	(14)
$S_2O_3^{2-} + Zn^{2+} \rightarrow ZnS_2O_3$	2.3	(15)
$S_2O_3^{2-} + Fe^{2+} \rightarrow FeS_2O_3^+ + e^-$	-11.04	(16)
$S_2O_3^{2-} + Pb^{2+} \rightarrow PbS_2O_3$	5.634	(17)

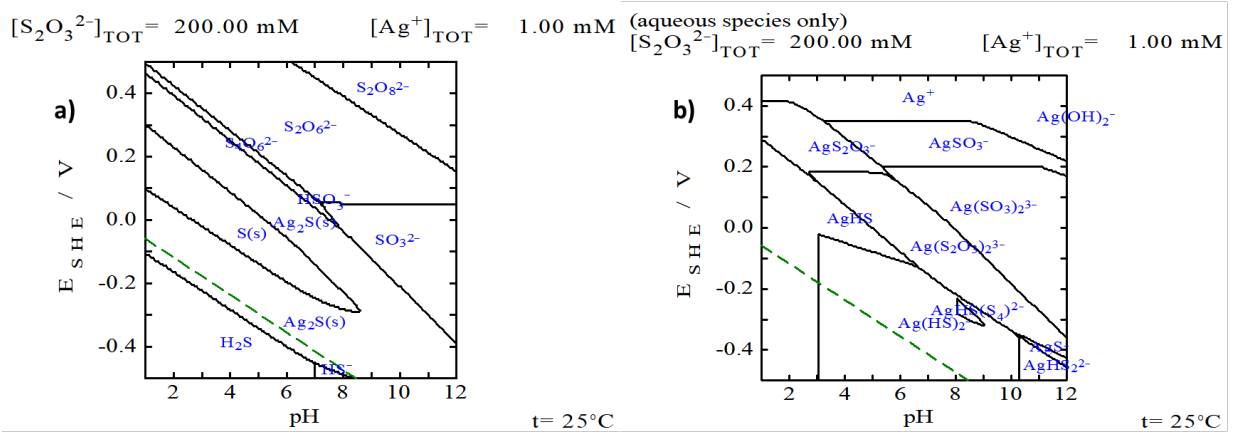

Figure 1 Eh–pH Diagram of the $S_2O_3^{2-}$–Ag system.

as silver sulfite. Similarly, the Pourbaix diagram in Figure (3a) shows the formation of the $CuS_2O_3^-$ complex, which is stable under the same Eh and pH conditions as the thiosulfate–silver complexes, highlighting the competition between Cu^{2+} and Ag^+ ions for the complexing agent. At reducing potentials and neutral to alkaline pH, solids such as CuS and Cu_2S are formed, evidencing copper precipitation. Previous studies indicate that Cu^{2+} ions act as catalysts in silver leaching with thiosulfate; however, chelating agents such as NH_3 (ammonia), EDTA (ethylenediaminetetraacetic acid), and MEA (monoethanolamine) have been used. These agents stabilize copper ions and prevent their precipitation, optimizing the efficiency of the process (Bruez *et al.*, 2024; Puente *et al.*, 2013; 2017; 2021; Xiang *et al.*, 2020; Rezaee *et al.*, 2023). Finally, thiosulfate decomposition produces S^0 (elemental sulfur), which can passivate the mineral surface.

In the Zn^{2+}–S_2O_3–Ag system (Figure 2b), the $Ag(S_2O_3)_2^{3-}$ complex predominates at pH ≈ 8 and moderately oxidizing potentials, but a lower concentration of thiosulfate is required compared to the system in the presence of Cu^{2+}. Although the formation of the ZnS_2O_3 complex is observed (Figure 3b), its stability zone is limited due to its lower equilibrium constant (log K = 2.33, Eq. 15) compared to $CuS_2O_3^-$ (log K = 12.93, Eq. 10). Furthermore, under reducing conditions and neutral to alkaline pH, ZnS precipitates are observed, while in more oxidizing environments, ZnO may form.

In the S_2O_3–Ag–Fe^{2+} system (Figure 2c), the stability of the $Ag(S_2O_3)_3^{5-}$ complex is more limited compared to the Cu^{2+} system, due to a greater tendency for thiosulfate oxidation, which favors the formation of $Ag(SO_3)_2^{3-}$ and reduces the stability of the thiosulfate–silver complex. On the other hand, the formation of the FeS_2O_3 complex is not thermodynamically favored (log K = -11.04, Eq. 16),

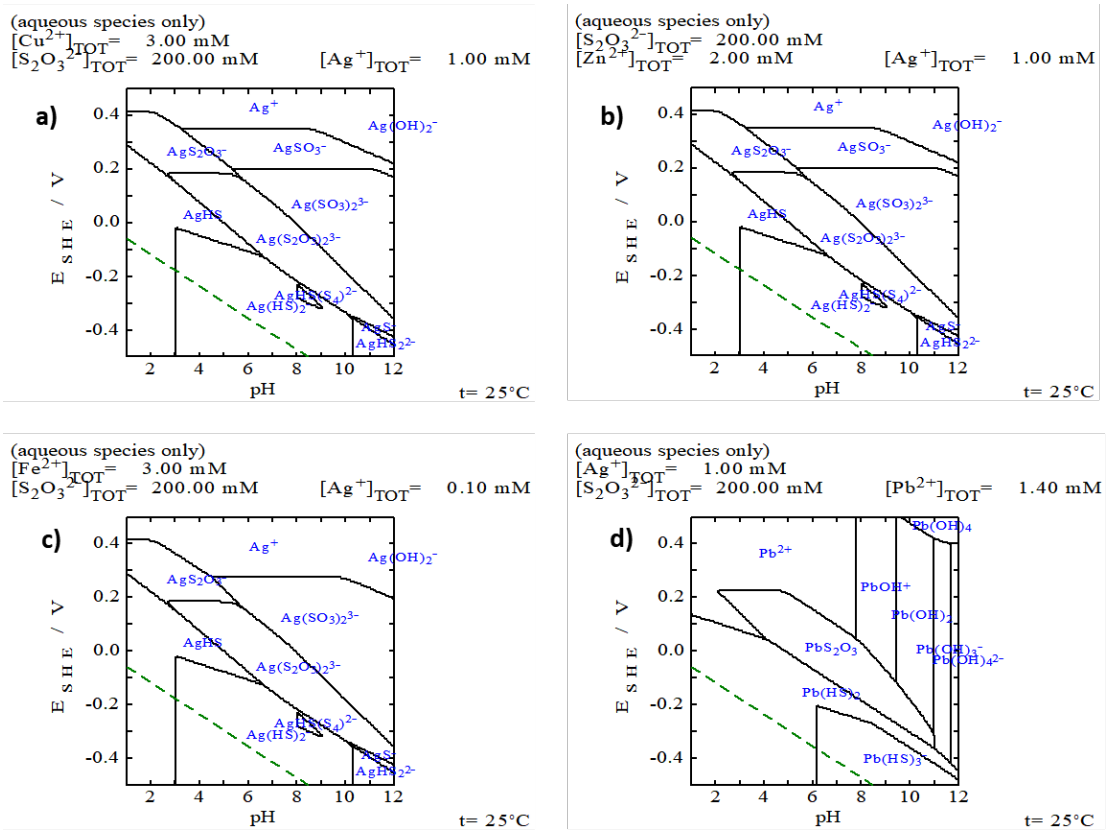

Figure 2. Eh-pH diagrams (aqueous species) of the systems: a) S_2O_3-Ag-Cu^{2+}, b) S_2O_3-Ag-Zn^{2+}, c) S_2O_3-Ag-Fe^{2+}, d) S_2O_3-Ag-Pb^{2+}.

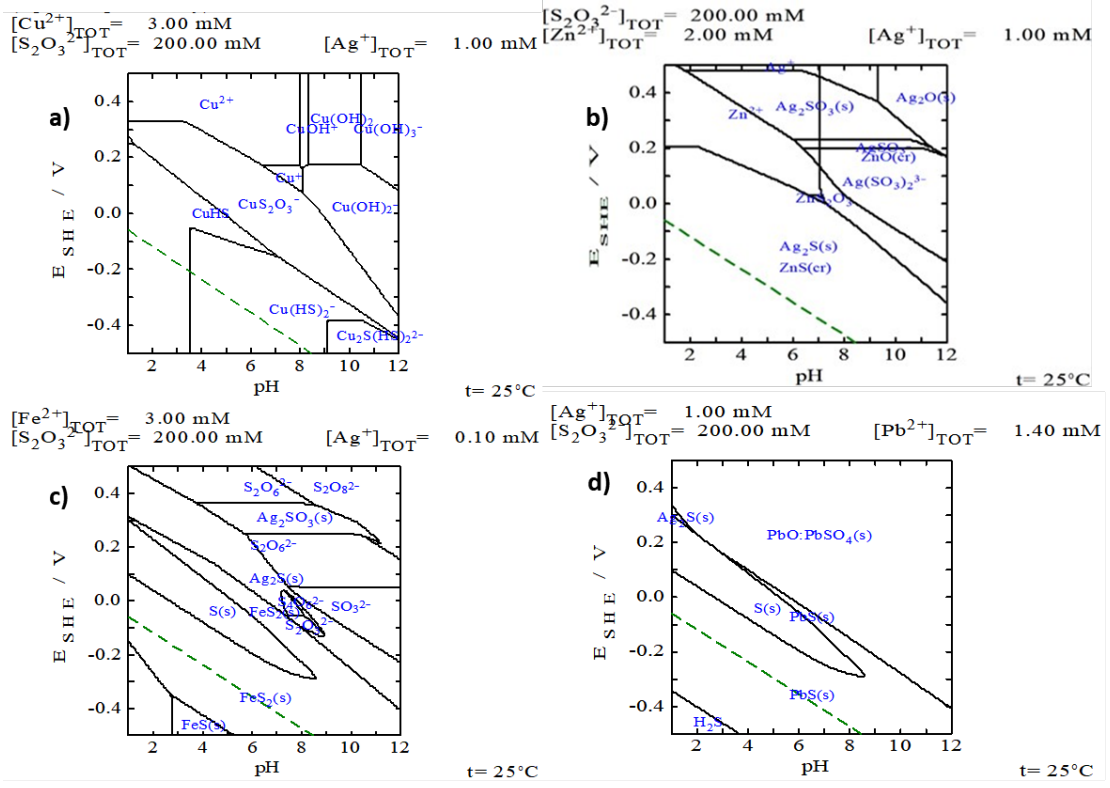

Figure 3 Eh–pH Diagrams of the Systems: a) S_2O_3–Ag–Cu^{2+}, b) S_2O_3–Ag–Zn^{2+}, c) S_2O_3–Ag–Fe^{2+}, d) S_2O_3–Ag–Pb^{2+}.

indicating an unlikely reaction. Instead, species such as HSO_3^- and SO_3^{2-} predominate (Figure 3c). The formation of HSO_3^- is significant, as its acidic nature can reduce the system's pH, altering the experimental conditions and accelerating the decomposition of thiosulfate in the presence of Fe^{2+}.

Finally, the predominant phases of the S_2O_3–Ag–Pb^{2+} system are shown (Figures 2 and 3d). The $AgS_2O_3^-$ and $Ag(S_2O_3)_3^{5-}$ complexes are stable in the presence of Pb^{2+}; however, the PbS_2O_3 complex (Eq. 17) is also formed under similar Eh and pH conditions, suggesting competition between Ag^+ and Pb^{2+} ions for the complexing agent, potentially decreasing the efficiency of Ag leaching. Additionally, under reducing conditions, PbS precipitates are formed, while in oxidizing environments, $PbO \cdot PbSO_4$ is observed (Figure 3d).

3.2 *Leaching tests*

The following section presents the analysis of the effect of different metallic ions (Cu^{2+}, Zn^{2+}, Fe^{2+}, Pb^{2+}) on silver sulfide leaching in the S_2O_3–air–OH system.

3.2.1 *Effect of Cu^{2+} concentration*

Figure 4 shows the performance of AgS dissolution in the presence of Cu^{2+} ions at different concentrations. It is observed that lower concentrations of $CuSO_4$ (0.062 and 0.187 g/L) allow achieving the highest silver leaching percentages, reaching 45.63% at 12 hours and 41.33% at 24 hours, respectively. In contrast, increasing the concentration in the range of 0.25 to 1.0 g/L results in a decrease in silver dissolution, with percentages lower than those obtained in the absence of Cu^{2+}. Concentrations of 0.75 and 1.0 g/L led to the lowest recovery values, reaching only 16.17% and 18.10%, respectively. Additionally, the slopes of the curves corresponding to the lower $CuSO_4$ concentrations are steeper, reflecting a higher dissolution rate.

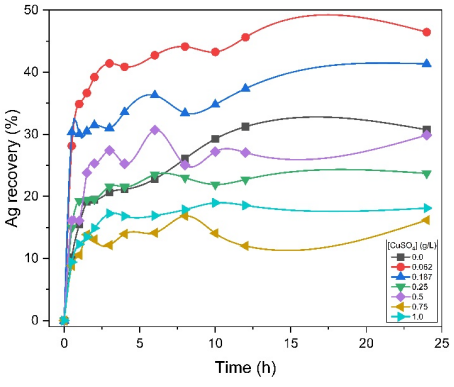

Figure 4 Silver sulfide leaching in the presence of Cu^{2+} ions.

The limitation in the maximum dissolution percentage of silver sulfide can be attributed to the partial decomposition of the complexing agent, followed by undesirable reactions that reduce the contact between the leaching solution and the Ag_2S surface, preventing the complete reaction and dissolution of the sample (eq 23-24).

3.2.2 *Effect of Zn^{2+} concentration*

Figure 5 illustrates the silver sulfide leaching behavior in the presence of different concentrations of zinc sulfate. During the first hour, the percentages of leached silver range between 27% and 33%, reflecting a rapid response of the system to the presence of Zn^{2+} and suggesting a very short or non-existent induction period. This allows the process to progress directly toward the conversion and stability phases. Specifically, concentrations of 0.33 g/L and 0.55 g/L of $ZnSO_4$ showed a sustained increase in silver sulfide dissolution between 12 and 24 hours, reaching a maximum value of 37.83% with 0.33 g/L. This behavior aligns with the findings of Juárez *et al.* (2012), who reported that the presence of Zn^{2+} enhances the silver dissolution rate with thiosulfate. Although the other concentrations analyzed show dissolution percentages similar to the system without Zn^{2+}, none resulted in a value lower than the 30.72% observed in the absence of this ion. Overall, Ag dissolution values remained between 30.8% and 33.76%. These results suggest that, while the increase in silver leaching is not significant, the process rate is notably higher, which implies a reduction in the resources required during experimentation.

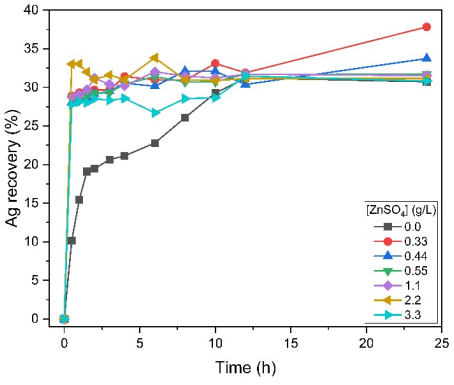

Figure 5 Silver sulfide leaching in the presence of Zn^{2+} ions.

3.2.3 *Effect of Fe^{2+} concentration*

Figure 6 shows the effect of different $FeSO_4$ concentrations (0.0 to 2.0 g/L) on silver sulfide leaching. In the absence of Fe^{2+} (0.0 g/L), a leaching percentage of approximately 35% was achieved after 12 hours of reaction, maintaining good stability

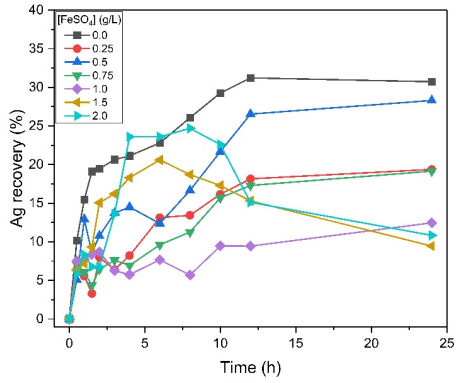

Figure 6 Silver sulfide leaching in the presence of Fe^{2+} ions.

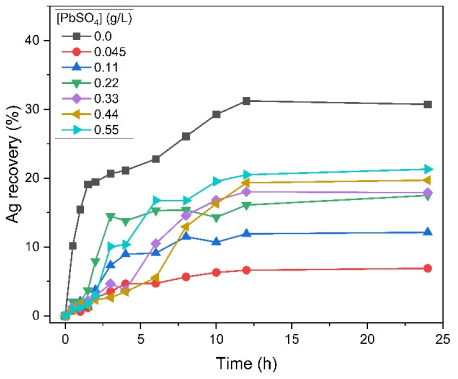

Figure 7 Silver sulfide leaching in the Presence of Pb^{2+} ions.

over time. However, the addition of Fe^{2+} negatively impacted both silver recovery and process stability (pH < 6), with effects varying according to the concentration used. At $FeSO_4$ concentrations between 1.0 and 2.0 g/L, a decrease in process efficiency was observed. At 1.0 g/L, the maximum recovery was 12.4%, while concentrations of 1.5 and 2.0 g/L resulted in values decreasing to 10% and 9%, respectively, after 5 hours. The presence of Fe^{2+} resulted in lower silver leaching efficiencies compared to its absence. This effect is attributed to the thiosulfacide behavior of Fe^{2+} ions, which alter the experimental conditions by increasing the oxidation-reduction potential (ORP) and promoting iron hydrolysis, leading to a gradual decrease in pH. According to Xu *et al.* (2017), the reduction in pH accelerates thiosulfate decomposition, forming elemental sulfur and other sulfur species, thereby reducing the availability of the leaching agent. This phenomenon explains the lower silver recovery observed under these conditions.

3.2.4 *Effect of Pb^{2+} concentration*

Figure 7 shows the effect of different $PbSO_4$ concentrations on silver sulfide dissolution with thiosulfate. In all cases, Ag_2S dissolution in the presence of Pb^{2+} was lower compared to the system without this ion. The maximum silver leaching percentage, 21.3%, was achieved after 24 hours of reaction with a $PbSO_4$ concentration of 0.55 g/L. At lower concentrations, such as 0.045 g/L of $PbSO_4$, silver recovery decreased significantly, reaching only 6.89% over the same period. This behavior suggests that the presence of lead has a significant inhibitory effect on silver sulfide leaching. Overall, the presence of Pb^{2+} not only limits silver sulfide dissolution but also slows down the process, acting as a thiosulfacide cation.

Given that the presence of certain ions in thiosulfate-based leaching systems can negatively affect silver extraction, the implementation of a staged leaching process is suggested. This approach would allow for the selective removal of species that may act as thiosulfate consuming agents, either by decomposing thiosulfate, generating undesirable reactions, or increasing its consumption (Ruíz & Lapidus, 2017). Table 3 presents several systems that have been studied with the aim of selectively extracting some of these cations.

3.3 *Characterization of solid residues by XRD*

The solid residues analyzed correspond to the precipitates obtained directly from the leaching experiments, which were subsequently filtered and dried before characterization.

3.3.1 *$Ag_2S - S_2O_3 - Cu$ system*

Figure 8 shows the diffractogram of the solid residues obtained during the silver sulfide leaching process with thiosulfate in the presence of Cu^{2+} ions. Characteristic peaks of silver sulfide (Ag_2S), copper(II) sulfide (CuS), copper(II) oxide (CuO), and elemental sulfur (S) are observed.

The reaction mechanism for silver sulfide leaching in the Ag_2S–$S_2O_3^{2-}$–Cu^{2+} system is based on the species identified through XRD, thermodynamic analysis, and experimental results. This mechanism is described as follows:

Silver sulfide dissociates (Eq. 18), releasing silver ions (Ag^+) and sulfide S^{2-}, which can subsequently be converted to elemental sulfur either by oxidation (Eq. 19) or through thiosulfate decomposition.

$$Ag_2S \rightarrow 2Ag^+ + S^{2-} \quad (18)$$

$$S^{2-} \rightarrow S^0 + 2e^- \quad (19)$$

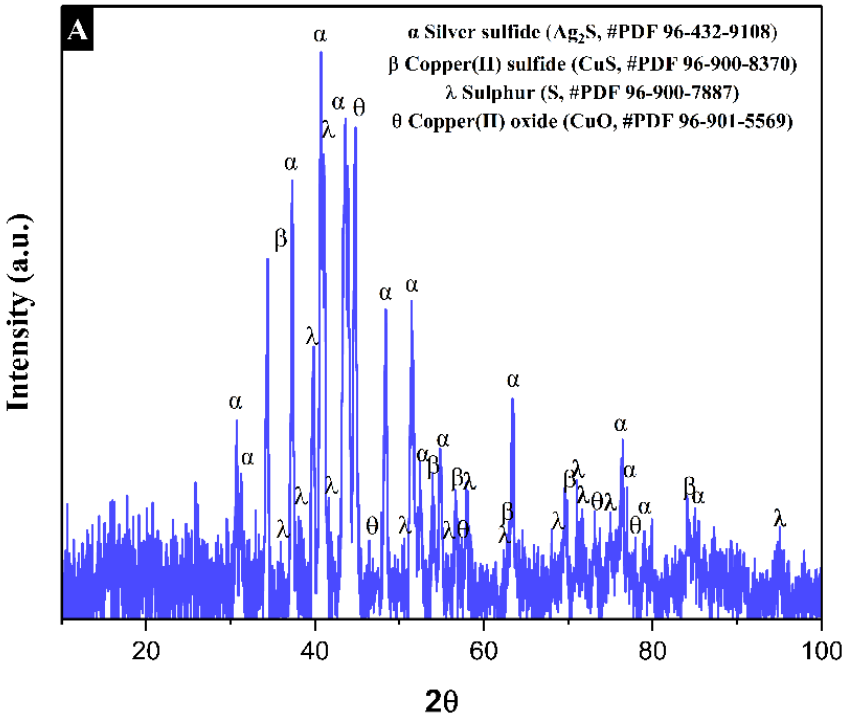

Figure 8 Diffractogram of the Leaching Residues from the Ag_2S–$S_2O_3^{2-}$–Cu System.

Table 3 Comparative Analysis of Selective Leaching Systems for Iron, Copper, Zinc, and Lead from Different Mineral Phases.

Element	Phase	System used	Reference
Iron (Fe) and Copper (Cu)	Chalcopyrite ($CuFeS_2$)	Two-stage leaching: (1) Oxalic acid + H_2O_2 to selectively dissolve iron, leaving copper in the matrix; (2) H_2SO_4 + H_2O_2 + ethylene glycol to extract copper without iron interference.	Ruiz-Sánchez & Lapidus, 2022
Copper (Cu)	Cuprite (Cu_2O) and Tenorite (CuO)	Advanced oxidation with sulfate radicals ($Na_2S_2O_8$) + acidic leaching.	Zuo *et al.*, 2023
Iron (Fe) and Lead (Pb)	Galena (PbS) and Pyrite (FeS_2)	Sodium citrate + H_2O_2 at pH 8 to selectively dissolve lead, followed by (2) pH adjustment to 5 to dissolve iron.	Torres & Lapidus, 2020; Calla *et al.*, 2024
Zinc (Zn)	Sphalerite, Wurtzite, and ZnO	H_2SO_4 at 90°C (a), at 30 °C (b)	(a) Xin *et al.*, 2022, (b) Borda *et al.*, 2021
Iron (Fe)	Goethite (FeOOH), Hematite (Fe_2O_3), Magnetite (Fe_3O_4)	H_2SO_4 + SO_2 / Organic acids (citric, oxalic)	Senanayake *et al.*, 2011
Zinc (Zn)	Sphalerite	Citrate – $Fe(NO_3)_3$ at 90°C	Nikkhou *et al.*, 2019
Lead (Pb)	Cerrusite ($PbCO_3$), Anglesite ($PbSO_4$)	EDTA at 25°C	Fin-gar & Letan, 2007
Zinc (Zn)	ZnO	Ultrasound-Enhanced NH_3-NH_4Cl-H_2O	Ma *et al.*, 2024

The available Ag ions (Eq. 18) can form complexes with thiosulfate in solution, as shown in Eq. 20. The $Ag(S_2O_3)_3^{5-}$ complex is the predominant phase indicated in Figure 2, considering the process described in Eq. 19:

$$2Ag^+ + 6S_2O_3^{2-} \rightarrow 2Ag(S_2O_3)_3^{5-} + S^0 + 2e^- \quad (20)$$

In parallel, dissolved oxygen is reduced to partially produce hydrogen peroxide (Eq. 21), which is subsequently reduced to produce OH^- ions (Eq. 22):

$$O_{2(ac)} + 2H_2O + 2e^- \rightarrow H_2O_2 + 2OH^- \quad (21)$$

$$H_2O_2 + 2e^- \rightarrow 2OH^- \quad (22)$$

On the other hand, Cu^{2+} ions in solution react with thiosulfate to form the $CuS_2O_3^-$ complex, as shown in Eq. 23. Additionally, these ions can react with the generated products to form copper(II) oxide (CuO) and copper(II) sulfide (CuS), as reported by Senanayake (2005), which are the result of thiosulfate decomposition into elemental sulfur (S^0) and sulfate (SO_4^{2-}), as described in Eqs. 24 and 25.

$$Cu^{2+} + S_2O_3^{2-} + e^- \rightarrow CuS_2O_3^- \quad (23)$$

$$Cu^{2+} + S_2O_3^{2-} + 2OH^- \rightarrow CuS_{(s)} + SO_4^{2-} + H_2O \quad (24)$$

$$Cu^{2+} + 2OH^- \rightarrow CuO + H_2O \quad (25)$$

Considering Eqs. 20 to 25, the following overall equation is proposed to describe the thiosulfate–silver sulfide–copper system (Eq. 26):

$$5Ag_2S + 33S_2O_3^{2-} + 4Cu^{2+} + 2O_2 + 2H_2O \rightarrow 10Ag(S_2O_3)_3^{5-} + 2CuS_2O_3^- + CuO + CuS_{(s)} + 5S + SO_4^{2-} + 4OH^- \quad (26)$$

Numerous studies support the use of Cu^{2+} ions as catalysts in silver leaching, highlighting their ability to enhance precious metal dissolution (Benijamali *et al*., 2021). However, the effectiveness of this catalyst critically depends on its concentration in the leaching solution. At elevated concentrations, undesirable reactions occur, including the formation of copper–thiosulfate complexes and precipitates such as CuS, CuO, and elemental sulfur (S^0), which may deposit on the Ag_2S surface and form passivating layers that hinder reactivity—thereby limiting process efficiency even in the presence of excess lixiviant. Furthermore, in continuous or closed systems, CuO accumulation within the leaching circuit can alter process dynamics and compromise both chemical stability and silver recovery. The findings of this study provide key insights into the dual role of Cu^{2+} in these systems and inform strategies to mitigate its adverse effects. For instance, the use of chelating agents such as EDTA can prevent precipitate formation, while sequential copper removal or the addition of stabilizing agents like ammonia or glycine may enhance overall system performance (Barrios *et al*., 2024; Bruez *et al*., 2024; Hao *et al*., 2023).

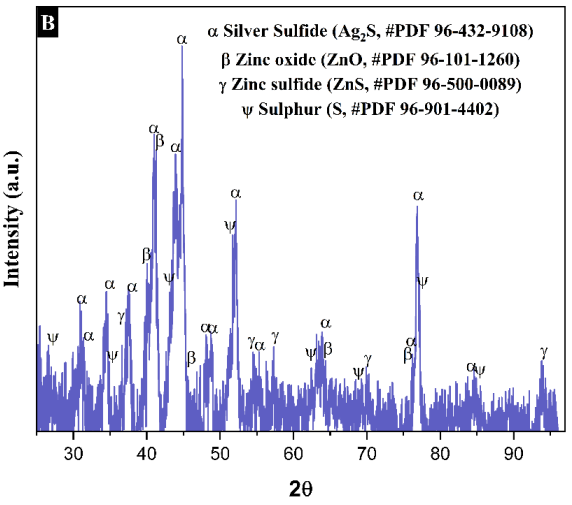

Figure 9 Diffractogram of the Leaching Residues from the Ag_2S–$S_2O_3^{2-}$– Zn System.

3.3.2 $Ag_2S - S_2O_3 - Zn$ system

The diffractogram corresponding to the solid residues of the $S_2O_3^{2-}$–Ag_2S–Zn^{2+} system, presented in Figure 9, reveals characteristic peaks of silver sulfide (Ag_2S), which did not react with the leaching agent, zinc oxide (ZnO), zinc sulfide (ZnS), and elemental sulfur (S).

The dissociation process proceeds as shown in Eqs. 18 and 19. According to the thermodynamic study, Ag^+ ions form complexes with thiosulfate in solution in the presence of Zn^{2+} ions (Figure 2b), as shown in Eq. (27). In parallel, Zn^{2+} ions and thiosulfate react according to Eq. (28) (Figure 3b):

$$2Ag^+ + 4S_2O_3^{2-} \rightarrow 2Ag(S_2O_3)_2^{3-} + S^0 + 2e^- \quad (27)$$

$$Zn^{2+} + S_2O_3^{2-} + 2OH^- \rightarrow ZnS + SO_4^{2-} + H_2O \quad (28)$$

In turn, zinc in solution reacts with hydroxide ions (OH^-) to form zinc hydroxides ($Zn(OH)_4^{2-}$), as described in Eqs. 29 and 30. However, Eq. 31 outlines how the reaction in Eq. 30 leads to the formation of zinc oxide (ZnO) (Ismail *et al*., 2016):

$$O_2 + 2H_2O + 4e^- \rightarrow 4OH^- \quad (29)$$

$$Zn + 4OH^- \rightarrow Zn(OH)_4^{2-} + 2e^- \quad (30)$$

$$Zn(OH)_4^{2-} \leftrightarrow ZnO + H_2O + 2OH^- \quad (31)$$

From Eqs. 27 to 31, the overall equation for the S_2O_3–Ag_2S–Zn system in solution is established (Eq. 32). It is noteworthy that the required S_2O_3:Ag_2S ratio in this case is 5:1, which is lower than that of the copper system (6.6:1). This finding explains the higher initial reaction rate, as the consumption of the complexing agent is lower. Consequently, the concentration of thiosulfate becomes particularly relevant as a critical

factor in the leaching of precious metals (Godigamuwa & Okibe, 2023).

$$Ag_2S + 2ZnSO_4 + 5S_2O_3^{2-} + O_2 \rightarrow 2Ag(S_2O_3)_2^{3-} + ZnS + ZnO + S + 3SO_4^{2-} \quad (32)$$

Unlike Cu^{2+}, Zn^{2+} ions exhibit low thermodynamic affinity for thiosulfate, which limits its degradation and enhances the stability of the complexing agent. This creates a more favorable chemical environment, allowing for a faster initial leaching rate compared to other systems, such as that involving copper. However, despite this favorable kinetics, silver extraction stabilizes at moderate levels. This behavior suggests that the limiting factor is not thiosulfate availability, but the gradual formation of products such as ZnS and elemental sulfur (S^0), which deposit into the Ag_2S surface. These species may form passivating layers that hinder the lixiviant's access to the mineral, acting as kinetic barriers that restrict further leaching. As a result, even in chemically active conditions, the surface reactivity of Ag_2S becomes compromised, leading to a self-limiting process. At the industrial level, controlling parameters such as Zn^{2+} concentration, pH, and redox potential is critical to minimizing the precipitation of interfering species. If these effects are significant, strategies like the HNO_3–Fe^{3+}–citrate system (Nikkhou *et al.*, 2019) can be applied for selective zinc removal prior to silver leaching.

3.3.3 $Ag_2S - S_2O_3 - Fe$ system

In Figure 10, corresponding to the diffractogram of the leaching residues of Ag_2S in the presence of Fe, phases corresponding to Ag_2S, FeO_2H, and S were identified.

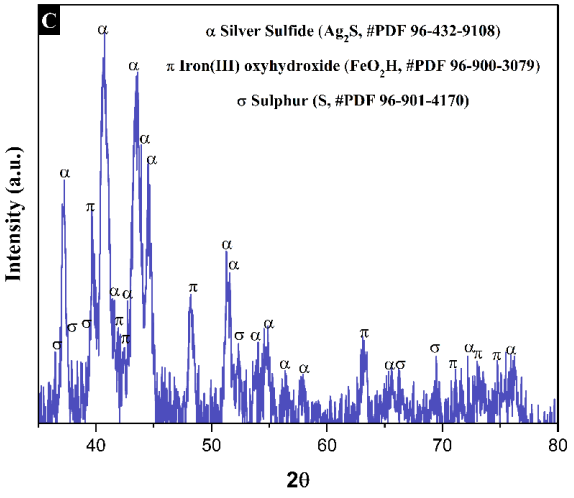

Figure 10 Diffractogram of the Leaching Residues from the S_2O_3–Ag_2S–Fe System.

In this case, the dissociation of Ag_2S proceeds as described in Eqs. 18 and 19. Furthermore, as observed in the results of Figure 2c, the formation of the $Ag(S_2O_3)_3^{5-}$ complex is represented by Eq. 20. On the other hand, the oxidation of Fe(II) to Fe(III) occurs through a coupled hydrolysis and precipitation process, represented by Equation 33. This mechanism generates cationic species that explain the pH decrease observed during the experimental process (Tabakova *et al.*, 1996). Additionally, as this is a redox process in the presence of dissolved oxygen—directly injected into the system—the conversion of Fe^{2+} to Fe^{3+} contributes to the increase in the oxidation-reduction potential (ORP), by removing a reducing agent (Fe^{2+}) and forming more oxidizing species. This reaction is considered the predominant pathway in the system, as X-ray diffraction (XRD) analysis confirmed the presence of FeOOH as the stable solid product.

$$FeSO_4 + 2H_2O \rightarrow FeOOH + 3H^+ + SO_4^{2-} + e^- \quad (33)$$

Although ferric iron tends to hydrolyze and contribute to acidification of the medium, the system was not maintained under acidic conditions. On the contrary, periodic pH adjustments were made to keep it within a neutral to slightly alkaline range, favoring the formation of FeOOH over less stable phases. This explains the absence of Fe(OH)- in the solid residues and the prevalence of FeOOH as the dominant precipitate under buffered conditions. Nonetheless, under transient, locally acidic conditions, additional reactive pathways may occur, such as the hydrolysis equilibria of Fe^{2+}:

$$Fe^{2+} + H_2O \rightarrow Fe(OH)^+ + H^+ \quad (34)$$

$$Fe(OH)^+ + H_2O \rightarrow Fe(OH)_2 \quad (35)$$

$$8Fe^{2+} + 5O_2 + 14H_2O \rightarrow 8Fe(OH)_{3(s)} + 4H^+ \quad (36)$$

With the increase in acidity in the leaching system, the decomposition of the complexing agent is favored, as described in Eqs. 37 to 40. Simultaneously, Eq. 40 represents the reduction process of dissolved O_2 under the specific conditions of the system:

$$0.5S_2O_3^{2-} \rightarrow 2H^+ + HSO_3^- + 2e^- \quad (37)$$

$$3H^+ + 2e^- + 0.5S_2O_3^{2-} \rightarrow S_{(s)} \quad (38)$$

$$S_2O_3^{2-} + H^+ \rightarrow HSO_3^- + S_{(s)} \quad (39)$$

$$O_2 + 4H^+ + 4e^- \rightarrow 2H_2O \quad (40)$$

Considering the redox processes involved in the system, along with the degradation of the complexing agent due to the pH decrease, the overall equation for Ag leaching with thiosulfate in the presence of Fe^{2+} ions is proposed in Eq. 41:

$$4Ag_2S + 25S_2O_3^{2-} + 4Fe^{2+} + 2H_2O + 3O_2 + H^+ \rightarrow 8Ag(S_2O_3)_3^{5-} + 4FeOOH + HSO_3^- + 5S \quad (41)$$

Taken together, these processes, whether through direct oxidation of Fe^{2+} or partial hydrolysis, lead to localized acidification of the medium, which significantly compromises thiosulfate stability. The decomposition of the complexing agent under these conditions results in the generation of elemental sulfur (S^0), which may accumulate on the Ag_2S surface and form passivating layers that hinder further reaction. This dual effect, the loss of the active lixiviant and surface blockage, provides a compelling explanation for the low silver extraction observed in the presence of Fe^{2+}, which was the least efficient system despite the controlled pH conditions. At larger scales, Fe^{2+} presents substantial operational challenges due to its high reactivity in thiosulfate media. It disrupts the chemical equilibrium of the solution, accelerates lixiviant degradation, and promotes the formation of solid precipitates. These solids not only increase reagent consumption but also hinder silver recovery, complicate waste handling, and interfere with the control of key parameters such as pH and ORP. For this reason, strategies such as the oxalic acid–H_2O_2–ethyleneglycol system (Ruíz & Lapidus, 2020) are essential for selectively dissolving iron compounds, minimizing precipitate accumulation, and enhancing overall process stability in industrial applications.

3.3.4 $S_2O_3 - Ag_2S - Pb$ system

In the S_2O_3–Ag_2S–Pb^{2+} system, the analysis of solid residues by XRD (Figure 11) reveals the presence of phases such as silver sulfide (Ag_2S), lead oxide (PbO), lead sulfide (PbS), and elemental sulfur (S^0).

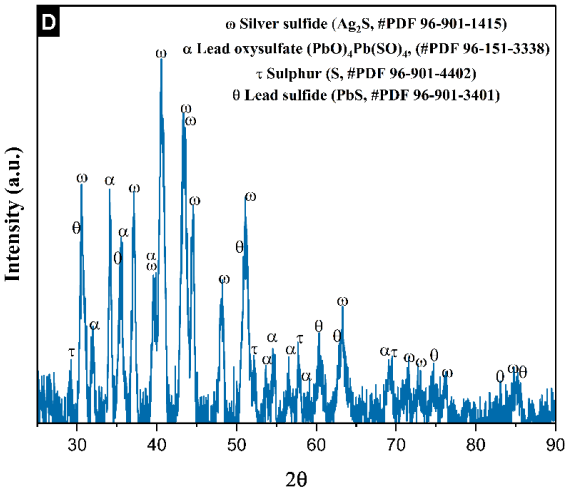

Figure 11 Diffractogram of the Leaching Residues from the S_2O_3–Ag_2S–Pb System.

These results suggest that the leaching process is strongly affected by secondary reactions that promote the formation of passivating layers. According to the thermodynamic analysis and the results in Figure 2d, silver ions form thiosulfate complexes as described in Eq. 20. Simultaneously, Pb^{2+} ions interact with thiosulfate to produce $PbO \cdot PbSO_4$, as shown in Eq. 42, contributing to the accumulation of stable solid phases.

$$S_2O_3^{2-} + 4Pb^{2+} + 7H_2O \rightarrow 2PbO \bullet PbSO_4 + 14H^+ + 8e^- \quad (42)$$

Considering the reduction of dissolved oxygen (Eq. 29), the net redox process is proposed in Eq. 43:

$$Ag_2S + 7S_2O_3^{2-} + 4PbSO_4 + 2.5O_2 + 2H_2O \rightarrow 2Ag(S_2O_3)_3^{5-} + 2PbO \bullet PbSO_4 + 4SO_4^{2-} + S + 4H^+ \quad (43)$$

On the other hand, thiosulfate decomposition in alkaline conditions, as reported by Melashvili *et al.* (2015), leads to the formation of sulfide ions (S^{2-}) and the oxidation of sulfite to sulfate (Eqs. 44 and 45). These species react with Pb^{2+}, precipitating as lead sulfide (PbS), as supported by Chen *et al.* (2014):

$$2S_2O_3^{2-} + 6OH^- \rightarrow 4SO_3^{2-} + 2S^{2-} + 3H_2O \quad (44)$$

$$SO_3^{2-} + 0.5O_2 \rightarrow SO_4^{2-} \quad (45)$$

$$S^{2-} + Pb^{2+} \rightarrow PbS \quad (46)$$

These reactions are consolidated in Eq. 47, which describes the mechanism of Ag_2S leaching in the presence of Pb^{2+}:

$$4Ag_2S + 10S_2O_3^{2-} + 6PbSO_4 + 4.5O_2 + 6OH^- \rightarrow 2Ag(S_2O_3)_3^{5-} + 2PbS + 2PbO \bullet PbSO_4 + 10SO_4^{2-} + S + 4H^+ + H_2O \quad (47)$$

The formation of PbS, $PbO.PbSO_4$, and elemental sulfur (S^0) indicates the development of passivating layers on the mineral surface that inhibit silver dissolution and reduce process efficiency. This is consistent with the results in Figure 7, where silver recovery appears limited despite the presence of excess thiosulfate. These passivating phases restrict the accessibility of the lixiviant to reactive sites, representing a major kinetic limitation.

In industrial applications, the presence of Pb^{2+} presents multiple challenges. It increases thiosulfate consumption through side reactions, complicates silver recovery due to co-precipitation, and reduces the purity of the final product. Furthermore, the persistence of Pb in leaching tailings raises environmental and regulatory concerns due to its toxicity. To mitigate these effects, Alonso & Lapidus (2009) proposed the addition of phosphate, which decreases Pb^{2+} solubility during leaching. Additionally, citrate-based leaching systems combined with hydrogen peroxide have been shown to selectively extract Pb while minimizing its interference in silver recovery, as demonstrated by Torres *et al.* (2018). Implementing such strategies

improves process efficiency and product quality while reducing environmental liabilities and treatment costs.

The results obtained in this study confirm the predictions made through the thermodynamic analysis. The Eh-pH diagrams (Section 3.1) provided insight into the stability regions of the silver-thiosulfate complexes and the potential interactions of Cu^{2+}, Zn^{2+}, Fe^{2+}, and Pb^{2+} in the system. These predictions were validated by the leaching experiments (Section 3.2), which demonstrated that Cu^{2+} at low concentrations and Zn^{2+} favor silver dissolution, while Fe^{2+} and Pb^{2+} negatively affect the process by promoting thiosulfate decomposition or forming passivating layers. The XRD analysis (Section 3.3) further confirmed these findings, identifying the formation of solid phases such as CuS, ZnO, FeOOH, and $PbO \cdot PbSO_4$, which were consistent with the species predicted in the thermodynamic modeling. These results highlight the importance of considering both thermodynamic stability and experimental validation when designing leaching processes for complex systems. Additionally, the information presented in Table 3 reinforces the relevance of selective dissolution approaches for problematic cations, providing a framework for optimizing multi-stage leaching strategies.

Conclusions

In this research, the effect of different metallic ions on the silver sulfide leaching process with thiosulfate was analyzed, yielding the following findings:

(1) The dual influence of Cu^{2+} in thiosulfate leaching was confirmed, acting as a catalyst at low concentrations and as a thiosulfacide species at higher concentrations. Its control is key to optimizing silver recovery.

(2) Zn^{2+} ions enhance the dissolution kinetics of Ag_2S without significantly affecting the final silver recovery, representing an advantage in terms of lixiviant stability and process efficiency.

(3) Fe^{2+} and Pb^{2+} exhibited negative effects on Ag leaching, promoting thiosulfate degradation and the formation of passivating layers, thereby reducing process efficiency.

(4) The efficiency of the silver sulfide leaching process is closely linked to the chemical stability of thiosulfate and the surface reactivity of the mineral. The generation of decomposition products such as elemental sulfur, as well as the precipitation of metal sulfides or oxides, can lead to passivating layers that inhibit the lixiviant–mineral interaction. This behavior, observed in systems containing Fe^{2+} and Pb^{2+}, is also evident with Cu^{2+} and Zn^{2+} at higher concentrations, where they contribute to thiosulfate degradation or surface passivation. These effects are analogous to the action of cyanide-consuming metals (cyanicides) in conventional leaching systems. Therefore, it is proposed that these interfering species be conceptually classified as "thiosulfacide metals," given their capacity to reduce silver recovery and their importance for guiding pre-treatment strategies in polymetallic ores.

Acknowledgements

The authors of this article extend their gratitude to the Universidad Autónoma del Estado de Hidalgo for providing the facilities required to conduct the experimentation. Additionally, they thank the Secretaría de Ciencia, Tecnología, Humanidades e Innovación (SeCiTHI)for the financial support provided.

References

Alarcon, A., Segura, C., Gamarra, C., & Rodriguez-Reyes, J. C. F. (2018). Green chemistry in mineral processing: chemical and physical methods to enhance the leaching of silver and the efficiency in cyanide consumption. Pure and Applied Chemistry, 90(7), 1109-1120. https://doi.org/10.1515/pac-2017-0904

Alonso, A. R., & Lapidus, G. T. (2009). Inhibition of lead solubilization during the leaching of gold and silver in ammoniacal thiosulfate solutions (effect of phosphate addition). Hydrometallurgy, 99(1-2), 89-96. https://doi.org/10.1016/j.hydromet.2009.07.010

Alvarado, G., Fuentes-Aceituno, J. C., & Nava-Alonso, F. (2015). Silver leaching with the thiosulfate–nitrite–sulfite–copper alternative system. Hydrometallurgy, 152, 120-128. https://doi.org/10.1016/j.hydromet.2014.12.017

Asencios, Y. J., Martínez, J. C., & Rodríguez, A. (2022). Biosorción de metales pesados utilizando algas marinas modificadas químicamente. Revista Mexicana de Ingeniería Química, 21(1), 157–170. https://rmiq.org/iqfvp/Numbers/V21/No1/IA2600.pdf

Barrios, J. M. H., Flores, G. C., Tapia, J. C. J., Ruíz, A. M. T., Ortiz, O. J. H., & García, F. L. (2024).

Efecto sinérgico de tiosulfato de sodio y glicina en la lixiviación de plata, utilizando peróxido de hidrógeno como oxidante y etilenglicol, en una muestra polimetálica de Zimapán: influencia de la temperatura. Tópicos de Investigación en Ciencias de la Tierra y Materiales, 11(11), 46-52. https://doi.org/10.29057/aactm.v11i11.13140

Borda, J., Torres, R., & Lapidus, G. Selective leaching of zinc and lead from electric arc furnace dust using citrate and H2SO4 solutions. A kinetic perspective Lixiviación selectiva de zinc y plomo del polvo de un horno de arco eléctrico utilizando soluciones de citrato y H2SO4. Una perspectiva cinética. https://doi.org/10.24275/rmiq/Cat2606

Bruez, C., Rousseau, A., Lefèvre, G., & Monteux, C. (2024). Investigation of the use of foams for silver leaching using the thiosulfate-copper (II)-ammonia system in the context of e-waste recycling. Hydrometallurgy, 225. https://doi.org/10.1016/j.hydromet.2024.106279

Calla, D., Pantaleón, D. M., & Lapidus, G. T. (2024). The fate of the sulfide ion in galena leaching with neutral citrate media. Revista Mexicana de Ingeniería Química, 23(3), Artículo IA24304. https://doi.org/10.24275/rmiq/IA24304

Chen, J. H., Li, Y. Q., Lan, L. H., & Guo, J. (2014). Interactions of xanthate with pyrite and galena surfaces in the presence and absence of oxygen. Journal of Industrial and Engineering Chemistry, 20(1), 268-273. https://doi.org/10.1016/j.jiec.2013.03.039

Cos, C. E., & Fuentes, J. C. (2023). Comprehensive Analysis of the Dissolution of Precious Metals with Innovative Amine-Based Leaching Systems. Epistemus (Sonora), 17(34), 32-40. https://doi.org/10.36790/epistemus.v17i34.267

Deutsch, J. L. (2012). Fundamental aspects of thiosulfate leaching of silver sulfide in the presence of additives (Doctoral dissertation, University of British Columbia). https://dx.doi.org/10.14288/1.0072556

Dwivedi, N., & Dwivedi, S. (2021). Sustainable biological approach for removal of cyanide from wastewater of a metal-finishing industry. In Membrane-Based Hybrid Processes for Wastewater Treatment (pp. 463-479). Elsevier. https://doi.org/10.1016/B978-0-12-823804-2.00010-0

Erust, C., Karacahan, M. K., & Uysal, T. (2023). Hydrometallurgical roadmaps and future strategies for recovery of rare earth elements. Mineral Processing and Extractive Metallurgy Review, 44(6), 436-450. https://doi.org/10.1080/08827508.2022.2073591

Godigamuwa, K., & Okibe, N. (2023). Gold leaching from printed circuit boards using a Novel Synergistic Effect of Glycine and Thiosulfate. Minerals, 13(10). https://doi.org/10.3390/min13101270

H.Y., Li., Elsayed, Oraby., Jacques, Eksteen. (2022). Development of an integrated glycine-based process for base and precious metals recovery from waste printed circuit boards. Resources Conservation and Recycling. https://doi.org/10.1016/j.resconrec.2022.106631

Hao, J., Wang, X., Wang, Y., Guo, F., & Wu, Y. (2023). Study of gold leaching from pre-treated waste printed circuit boards by thiosulfate-cobalt-glycine system and separation by solvent extraction. Hydrometallurgy, 221. https://doi.org/10.1016/j.hydromet.2023.106141

Hou, L., Valdivieso, A. L., Robledo-Cabrera, A., Zainiddinovich, N. Z., Wu, C., Song, S., & Jia, F. (2024). Stepwise oxidation of refractory pyrite using persulfate for efficient leaching of gold and silver by an eco-friendly copper (II)-glycine-thiosulfate system. Powder Technology, 448. https://doi.org/10.1016/j.powtec.2024.120323

Ismail, W. M. I. W., Zulkefeli, N. S. W., & Masri, M. N. (2016). A sight of zinc corrosion in various alkaline media. Journal of Tropical Resources and Sustainable Science (JTRSS), 4(2), 95-97. https://doi.org/10.47253/jtrss.v4i2.614

Juárez, Julio C, Rivera, Isauro, Patiño, Francisco, & Reyes, María I. (2012). Efecto de la Temperatura y Concentración de Tiosulfatos sobre la Velocidad de Disolución de Plata contenida en Desechos Mineros usando Soluciones S2O32--O2-Zn2+. Información tecnológica, 23(4), 133-138. https://dx.doi.org/10.4067/S0718-07642012000400015

Larrabure, G., & Rodríguez-Reyes, J. C. F. (2021). A review on the negative impact of different elements during cyanidation of gold and silver from refractory ores and strategies to optimize the leaching process. Minerals

Engineering, 173. https://doi.org/10.1016/j.mineng.2021.107194

Li, K., Li, Q., Zhang, Y., Liu, X., Yang, Y., & Jiang, T. (2023). Improved thiourea leaching of gold from a gold ore using additives. Hydrometallurgy, 222. https://doi.org/10.1016/j.hydromet.2023.106204

Liu, W., Li, W., Liu, W., Shen, Y., Zhou, S., & Cui, B. (2023). A new strategy for extraction of copper cyanide complex ions from cyanide leach solutions by ionic liquids. Journal of Molecular Liquids, 383. https://doi.org/10.1016/j.molliq.2023.122108

Ma, A., Li, J., Chang, J., & Zheng, X. (2024). Mechanism Analysis and Experimental Research on Leaching Zn from Zinc Oxide Dust with an Ultrasound-Enhanced NH3-NH4Cl-H2O System. Sustainability, 16(7). https://doi.org/10.3390/su16072901

Melashvili, M., Fleming, C., Dymov, I., Matthews, D., & Dreisinger, D. (2015). Equation for thiosulphate yield during pyrite oxidation. Minerals Engineering, 74, 105-111. https://doi.org/10.1016/j.mineng.2015.02.004

Meléndez-Sánchez, A. C., Hernández-Carmona, G., & López-Maldonado, E. A. (2022). Aislamiento y caracterización de microorganismos resistentes a metales pesados en jales mineros. Revista Mexicana de Ingeniería Química, 21(1), 191–204. https://rmiq.org/iqfvp/Numbers/V21/No1/Bio2700.pdf

Mitra, S. (2019). Depletion, technology, and productivity growth in the metallic minerals industry. Mineral economics, 32(1), 19-37. https://doi.org/10.1007/s13563-018-0165-8

Mystrioti, C., Kousta, K., Papassiopi, N., Adam, K., Taxiarchou, M., & Paspaliaris, I. (2024). Evaluation of Thiosulfate for Gold Recovery from Pressure Oxidation Residues. Materials Proceedings, 15(1). https://doi.org/10.3390/materproc2023015087

Nikkhou, F., Xia, F., & Deditius, A. P. (2019). Variable surface passivation during direct leaching of sphalerite by ferric sulfate, ferric chloride, and ferric nitrate in a citrate medium. Hydrometallurgy, 188, 201-215. https://doi.org/10.1016/j.hydromet.2019.06.017

Ou, Y., Yang, Y., Li, K., Gao, W., Wang, L., Li, Q., & Jiang, T. (2023). Eco-friendly and low-energy innovative scheme of self-generated thiosulfate by atmospheric oxidation for green gold extraction. Journal of Cleaner Production, 387. https://doi.org/10.1016/j.jclepro.2022.135818

Pearson, R. G. (1997). Ácidos y bases duros y blandos. Primera parte: principios fundamentales. Educación Química, 8(4), 208-215. https://doi.org/10.22201/fq.18708404e.1997.4.66600

Puente, D. M., Fuente, J. C., Nava, F., Uribe, A., Pérez, R., & Martínez, V. J. (2021). A phenomenological study of the silver sulfide passivation and oxidative degradation of thiosulfate in the thiosulfate-ammonia-copper-citrate leaching system. Hydrometallurgy, 200. https://doi.org/10.1016/j.hydromet.2020.105547

Puente, D. M., Fuentes, J. C., & Nava, F. (2013). A kinetic–thermodynamic study of silver leaching in thiosulfate–copper–ammonia–EDTA solutions. Hydrometallurgy, 134, 124-131. https://doi.org/10.1016/j.hydromet.2013.02.010

Puente, D. M., Fuentes, J. C., & Nava, F. (2017). An analysis of the efficiency and sustainability of the thiosulfate-copper-ammonia-monoethanolamine system for the recovery of silver as an alternative to cyanidation. Hydrometallurgy, 169, 16-25. https://doi.org/10.1016/j.hydromet.2016.12.003

Rezaee, M., Shafaei, S. Z., Abdollahi, H., Mohammadnejad, S., & Mabudi, A. (2023). An Experimental and DFT Study on Using the Thiosulfate–Glycine Complex as an Alternative Agent of Cyanide in the Gold Leaching Process. Journal of Sustainable Metallurgy, 9(3), 1239-1252. https://doi.org/10.1007/s40831-023-00726-w

Ruiz, Á., & Lapidus, G. T. (2017). Study of chalcopyrite leaching from a copper concentrate with hydrogen peroxide in aqueous ethylene glycol media. Hydrometallurgy, 169, 192-200. https://doi.org/10.1016/j.hydromet.2017.01.014

Ruiz, Á., & Lapidus, G. T. (2018). Improved process for leaching refractory copper sulfides with hydrogen peroxide in aqueous ethylene glycol solutions. In Extraction 2018: Proceedings of the First Global Conference on Extractive Metallurgy (pp. 1289-1298). Springer International Publishing. https://doi.org/10.1007/978-3-319-95022-8_105

Ruiz, A., & Lapidus, G. T. (2022). A study to understand the role of ethylene glycol in the oxidative acid dissolution of chalcopyrite. Minerals Engineering, 180. https://doi.org/10.1016/j.mineng.2022.107502

Ruiz, A., Lázaro, I., & Lapidus, G. T. (2020). Improvement effect of organic ligands on chalcopyrite leaching in the aqueous medium of sulfuric acid-hydrogen peroxide-ethylene glycol. Hydrometallurgy, 193. https://doi.org/10.1016/j.hydromet.2020.105293

Segura, B. & Lapidus, G. (2023). Importance of chemical pretreatment for base metals remotion and its effect on the selective extraction of gold from Printed Circuits Boards (PCBs). Revista Mexicana de Ingeniería Química, 22(2), 563–578. https://doi.org/10.24275/rmiq/IA2335

Senanayake, G. (2005). Gold leaching by thiosulphate solutions: a critical review on copper (II)–thiosulphate–oxygen interactions. Minerals Engineering, 18(10), 995-1009. https://doi.org/10.1016/j.mineng.2005.01.006

Senanayake, G., Childs, J., Akerstrom, B. D., & Pugaev, D. (2011). Reductive acid leaching of laterite and metal oxides—A review with new data for Fe (Ni, Co) OOH and a limonitic ore. Hydrometallurgy, 110(1-4), 13-32. https://doi.org/10.1016/j.hydromet.2011.07.011

Serap, Ubiç., Rasoul, Khayyam, Nekouei., V., Sahajwalla. (2024). A Two-Step Leaching Process Using Thiourea for the Recovery of Precious Metals from Waste Printed Circuit Boards. https://doi.org/10.3390/waste2030018

Serga, V., Zarkov, A., Blumbergs, E., Shishkin, A., Baronins, J., Elsts, E., & Pankratov, V. (2022). Leaching of gold and copper from printed circuit boards under the alternating current action in hydrochloric acid electrolytes. Metals, 12(11). https://doi.org/10.3390/met12111953

Soto-Uribe, J. C., Valenzuela-Garcia, J. L., Salazar-Campoy, M. M., Parga-Torres, J. R., Vazquez-Vazquez, V. M., Encinas-Romero, M. A., & Martinez-Ballesteros, G. (2023). Electrocoagulation process for recovery of precious metals from cyanide leachates using a low voltage. ACS Engineering Au, 4(1), 139-144. https://doi.org/10.1021/acsengineeringau.3c00041

Tabakova, T., & Andreeva, D. (1996). Mechanism of the oxidative hydrolysis of Iron (II) sulphate. Bulgarian chemical communications, 29(2), 172-187. https://doi.org/10.1007/BF00703026

Torres, R., & Lapidus, G. T. (2020). Base metal citrate pretreatment of complex ores to improve gold and silver leaching with thiourea. Hydrometallurgy, 197. https://doi.org/10.1016/j.hydromet.2020.105461

Torres, R., Segura, B., & Lapidus, G. T. (2018). Effect of temperature on copper, iron and lead leaching from e-waste using citrate solutions. Waste management, 71, 420-425. https://doi.org/10.1016/j.wasman.2017.10.029

Trachevskii, V. V., Zimina, S. V., & Rodina, E. P. (2008). Thiosulfate metal complexes. Russian Journal of Coordination Chemistry, 34, 664-669. https://doi.org/10.1134/S1070328408090066

Urzúa, D. A., Fuentes, J. C., Uribe, A., & Lee, J. C. (2018). An electrochemical study of silver recovery in thiosulfate solutions. A window towards the development of a simultaneous electroleaching-electrodeposition process. Hydrometallurgy, 176, 104-117. https://doi.org/10.1016/j.hydromet.2018.01.017

Xiang, P. Z., Deng, C., Yao, H., Liu, L. J., & Mogdal, S. (2020, August). Leaching Kinetics of Gold Involved in the System S2O32--EDTA-Cu2+. In Materials Science Forum (Vol. 1001, pp. 212-218). Trans Tech Publications Ltd. https://doi.org/10.4028/www.scientific.net/MSF.1001.212

Xin, C., Xia, H., Jiang, G., Zhang, Q., Zhang, L., & Xu, Y. (2022). Studies on Recovery of Valuable Metals by Leaching Lead–Zinc Smelting Waste with Sulfuric Acid. Minerals, 12(10). https://doi.org/10.3390/min12101200

Xu, B., Kong, W., Li, Q., Yang, Y., Jiang, T., & Liu, X. (2017). A review of thiosulfate leaching of gold: Focus on thiosulfate consumption and gold recovery from pregnant solution. Metals, 7(6). https://doi.org/10.3390/met7060222

Yae, S., Iwai, Y., Takashima, Y., Osaka, T., & Matsumoto, A. (2023, December). Gold Recovery from Thiosulfate Leaching Solution Using Silicon Powder and Electrochemical Monitoring of Its Process. In Electrochemical Society Meeting Abstracts 244 (No. 25, pp.

1363-1363). The Electrochemical Society, Inc. https://doi.org/10.1149/MA2023-02251363mtgabs

Zhang, Y., Li, Q., Liu, X., & Jiang, T. (2022). A thermodynamic analysis on thiosulfate leaching of gold under the catalysis of Fe^{3+}/Fe^{2+} complexes. Minerals Engineering, 180. https://doi.org/10.1016/j.mineng.2022.107511

Zhang, Z. Y., Wu, L., He, K., & Zhang, F. S. (2022). A sequential leaching procedure for efficient recovery of gold and silver from waste mobile phone printed circuit boards. Waste Management, 153, 13-19. https://doi.org/10.1016/j.wasman.2022.08.011

Zuo, Q., Wu, D., Wen, S., Cao, J., Wang, Z., & Chen, H. (2023). Advanced oxidation using sulfate radicals for the surface oxidation of Cu_2O and the separation of copper via acid leaching. Journal of Molecular Liquids, 390. https://doi.org/10.1016/j.molliq.2023.123195